

Surface vibrational spectroscopy by infrared-visible sum frequency generation

X. D. Zhu, Hajo Suhr,* and Y. R. Shen

*Department of Physics, University of California, Berkeley, California 94720
and Materials and Molecular Research Division, Lawrence Berkeley Laboratory,
Berkeley, California 94720*

(Received 17 December 1986)

We report the first observation of a vibrational spectrum of a monolayer of molecular adsorbates by infrared-visible sum frequency generation. The results pave the way for future dynamic studies of surface phonons and molecular vibrations.

In the development of modern surface science, surface vibrational spectroscopy has played an essential role. It is important, for example, for *in situ* identification of adsorbates on surfaces and for understanding of interactions between adsorbates and between adsorbates and surfaces. This has led to the invention of a number of surface spectroscopic techniques; namely, electron-energy-loss spectroscopy,^{1,2} electron tunneling spectroscopy,¹ surface infrared spectroscopy,¹ surface photoacoustic spectroscopy,³ photodesorption spectroscopy,⁴ and surface picosecond Raman gain spectroscopy.⁵ However, none of these techniques are suitable for studies of fast surface molecular dynamics. Recently, optical second-harmonic generation has been proven to be a viable surface tool.⁶ Aside from the many advantages inherent to an optical probe, this technique is also capable of following surface modification with a subpicosecond time resolution.⁷ Naturally, one would like to extend the technique to infrared-visible sum frequency generation (SFG), since with the help of a tunable infrared laser, surface vibrational spectra as well as surface dynamics of selected adsorbates could then be studied via resonance-enhanced SFG. In this paper, we report the first step in that direction: the first successful attempt of recording a vibrational spectrum of a monolayer of molecules on a substrate by SFG.⁸

The basic idea of using SFG for vibrational spectroscopy is to convert the ir resonant signal to the visible so that it can be more easily detected. As a second-order process, SFG is forbidden in a bulk with centrosymmetry in the electric-dipole approximation, and therefore is highly surface specific.⁹ For the same reason, the ir resonances that can be probed by SFG must be both ir and Raman active. This is generally the case for surface modes because of the broken symmetry at the surface. Like second-harmonic generation (SHG), surface SFG has a signal strength proportional to the square of an effective surface nonlinear polarization⁹

$$\mathbf{P}_S^{(2)}(\omega = \omega_1 + \omega_2) = \vec{\chi}_S^{(2)} : \mathbf{E}(\omega_1)\mathbf{E}(\omega_2). \quad (1)$$

Close to a resonance, the effective surface nonlinear susceptibility $\chi_S^{(2)}$ can be written as

$$\vec{\chi}_S^{(2)} = \vec{\chi}_{NR}^{(2)} + \vec{\chi}_R^{(2)}, \quad \vec{\chi}_R^{(2)} = \sum_{\delta} A_{\delta} / (\omega_1 - \omega_{\delta} + i\Gamma_{\delta}), \quad (2)$$

where $\vec{\chi}_R^{(2)}$ and $\vec{\chi}_{NR}^{(2)}$ are the resonant and nonresonant

parts of $\vec{\chi}_S^{(2)}$, respectively, ω_{δ} is the resonant frequency, A_{δ} the strength, and Γ_{δ} the damping constant of the δ th mode. We assume here that the resonances originate from the surface adlayers. It can then be shown from the microscopic expression of $\vec{\chi}_R^{(2)}$ that

$$|\chi_R^{(2)}|^2 \sim |\chi_R^{(1)}\chi_R^{(3)}|, \quad (3)$$

where $\chi_R^{(1)}$ and $\chi_R^{(3)}$ are surface linear and Raman resonant susceptibilities, respectively, involving the same resonance. With typical values of $|\chi_R^{(1)}| \sim 10^{-8}$ esu and $|\chi_R^{(3)}| \sim 2 \times 10^{-20}$ esu,^{9,10} we have $|\chi_R^{(2)}| \sim 1.5 \times 10^{-14}$ esu. We therefore expect that the vibrationally resonant SFG should be observable since a surface susceptibility of $|\chi^{(2)}| \sim 10^{-15}$ esu is readily measurable in SHG.⁵

For demonstration, we used SFG to probe the vibrational modes of a monolayer of coumarin 504 molecules (Exciton Chemical Co., Inc.) spin-coated on a substrate of fused quartz.¹¹ The monolayer surface density of coumarin 504 was about 2×10^{14} /cm². To see that the technique could be applied to surface vibrational spectroscopy in the mid-ir range, we chose to study modes between 920 and 1100 cm⁻¹. This was achieved by overlapping an *s*-polarized frequency-doubled Nd:YAG (YAG denotes yttrium aluminum garnet) laser pulse at 0.532 μ m and a discretely tunable, *p*-polarized CO₂TEA (transversely excited atmospheric pressure) laser pulse operated at $\frac{1}{2}$ Hz on the sample. The susceptibility component measured was $\chi_{S,zy}^{(2)}$ with \hat{z} being the surface normal. The experimental setup is shown in Fig. 1. The reflected sum-frequency output from the surface was highly directional, and therefore, both spatial and spectral filtering could be used to help extract the signal. In order to minimize fluctuations due to shot-to-shot variations of laser intensities, mode structures, and pulse overlapping, the signal was properly normalized against the simultaneously monitored SF reflection from a GaAs(100) reference slab located in a side arm in the setup. The laser pulses impinging on the sample over a 7-mm² spot were 5 mJ/7 ns at 0.532 μ m and ~ 2 mJ/140 ns at the CO₂ laser wavelength. A photon counting detection system was used to record the signal. Typically, the signal strength was ~ 500 photons/pulse. The sample was constantly flushed with nitrogen during the experiment to slow down sample deterioration by oxidation.

In order to have an idea of what we would observe in SFG, we first measured ir, visible, and Raman spectra of

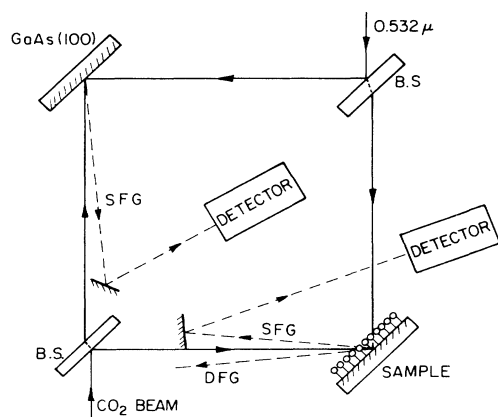


FIG. 1. Schematic diagram of experimental setup.

coumarin 504. Figure 2 depicts portions of the visible absorption spectrum of coumarin 504 in ethanol and the ir and Raman spectra of solid coumarin 504. From the spectra, it is seen that we should expect to observe in SFG a number of resonant vibrational structures in the range between 920 and 1100 cm^{-1} , where the tunability of our CO_2 laser could cover. The visible laser frequency (0.532 μm) we used sits on the shoulder of the visible absorption band of coumarin 504, so that some resonance enhancement in SFG should also be expected.

The results of our SFG experiment are shown in Fig. 3. The data points between 987 and 1025 cm^{-1} are missing because our CO_2 laser stopped lasing in that range. SFG is a coherent spectroscopic technique, and hence, the spectrum generally appears to be very different from the usual ir or Raman spectrum. To correlate the spectrum in Fig. 3 with the ir and Raman spectra in Fig. 2, we must keep in mind the following possible effects. (1) Interference between $\chi_{NR}^{(2)}$ and $\chi_R^{(2)}$ and between different terms in $\chi_R^{(2)}$ can distort the spectral line shape. (2) The frequencies of various vibrational modes are different for molecules adsorbed on a surface and for molecules in a solid. (3) The strengths of individual peaks may depend on the molecular orientation. Two resonant structures are clearly visible in the spectrum of Fig. 3. They can be identified with the infrared and Raman peaks around 950 and 1050 cm^{-1} . The infrared and Raman peaks around 920 and 1090 cm^{-1} cannot be resolved; they seem to have shifted just outside the spectral range we measured, so that only their shoulders appear in the spectrum of Fig. 3. The other infrared and Raman peaks at ~ 986 , 1016, and 1028 cm^{-1} also seem to have shifted out of the range we could reach.

With A_s , ω_s , and $\chi_{NR}^{(2)}$ taken as adjustable parameters, and Γ_s assumed to have the same values as the ir and Raman halfwidths in Fig. 2, Eq. (2) can be used to fit the experimental data. This is shown in Fig. 3. Knowing the collection efficiency of our detection system, we have obtained the absolute intensity of the SFG signal. The values of the parameters deduced from the fitting are listed in Table I. While those obtained from the partially observed resonances in Fig. 3 are not very accurate, those obtained for the two well-defined resonances are reasonably certain. The resonant frequencies are clearly shifted from those of

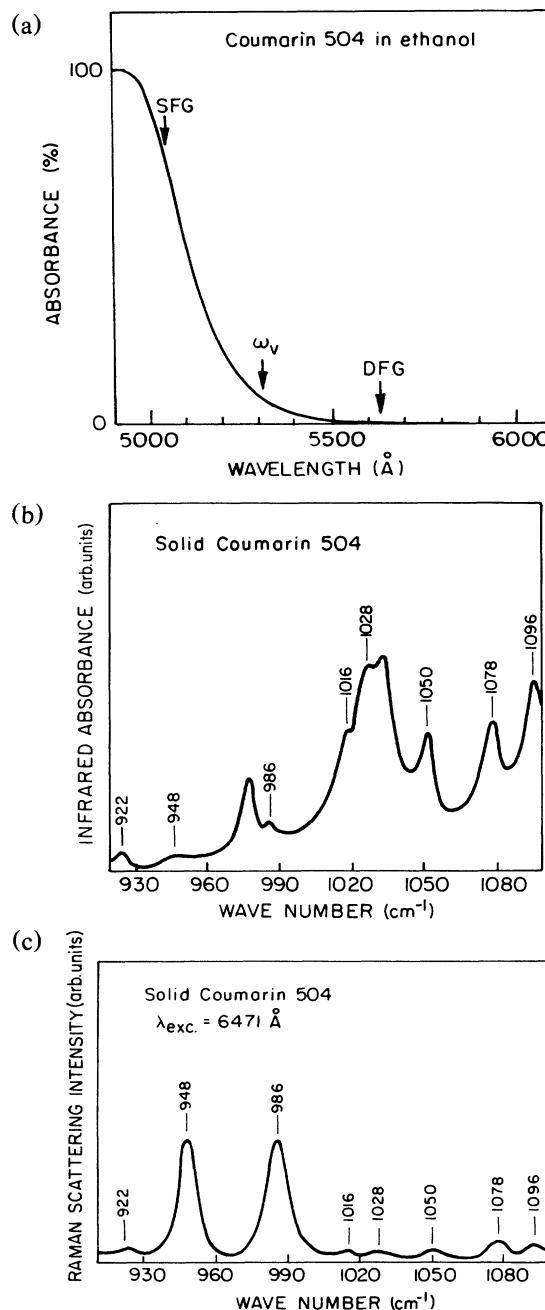


FIG. 2. (a) Visible absorption spectrum of coumarin 504 in ethanol, (b) infrared absorption spectrum, and (c) Raman spectrum of solid coumarin 504.

coumarin 504 in the solid phase as one might expect. Table I also shows that both $(\chi_R^{(2)})_{\text{max}}$ and $\chi_{NR}^{(2)}$ have values of the order of 10^{-14} esu. This agrees with our rough estimate given earlier.

For a better estimate of $(\chi_R^{(2)})_{\text{max}}$ of coumarin 504 for the ~ 1050 cm^{-1} mode, we calibrated the ir and Raman peaks of that mode in Fig. 2 with the corresponding 992- cm^{-1} mode of liquid pyridine. The ratios of $|\chi_R^{(1)}|_{\text{coumarin}}/|\alpha_R^{(1)}|_{\text{pyridine}}$, $|\chi_R^{(3)}|_{\text{coumarin}}/|\alpha_R^{(3)}|_{\text{pyridine}}$

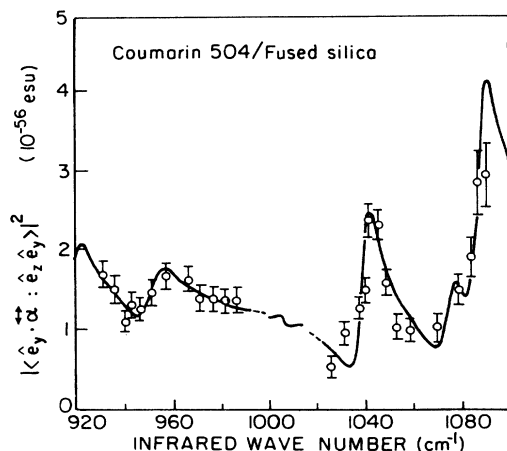


FIG. 3. Sum frequency vibrational spectrum of a monolayer of coumarin 504 on fused silica.

were found to be 1.0×10^{14} and 7.9×10^{14} esu, respectively, where α_R 's refer to molecular polarizabilities. For pyridine, it is known that $(\alpha_R^{(1)})_{\max} = 7.6 \times 10^{-24}$ esu and $(\alpha_R^{(3)})_{\max} = 3.1 \times 10^{-34}$ esu.¹² From Eq. (3), we then obtain for the 1050- cm^{-1} mode of coumarin 504, $(\chi_R^{(2)})_{\max} = 1.4 \times 10^{-14}$ esu. This compares well with the experimental value of $(\chi_R^{(2)})_{\max} = 1.8 \times 10^{-14}$ esu in Table I.

The large value of $\chi_{\text{NR}}^{(2)}$ can be understood knowing that coumarin 504 has many very strong ir and Raman modes in the range between 600 and 900 cm^{-1} and between 1100 and 1800 cm^{-1} . Their collective contribution would yield a large nonresonant background value for $\chi_S^{(2)}$. In the present case, the sum frequency is in the $S_0 \rightarrow S_1$ absorption band of coumarin. Therefore, $\chi_R^{(2)}$ and $\chi_{\text{NR}}^{(2)}$ should also be resonantly enhanced via the visible transition. To confirm this, we also conducted the difference-frequency ($\omega = \omega_1 - \omega_2$) generation experiment with the same setup. While the spectral feature resembled that of SFG, the output signal was ~ 10 times weaker.

One possible application of SFG spectroscopy to the studies of molecular adsorbates is to obtain information on the orientation of the adsorbates. This is particularly

effective when the sum frequency is also at resonance with an electronic transition. As in the case of SHG,¹³ the ratios of the various tensor components of $\chi^{(2)}$, measured by using proper polarization combinations in SFG, are functions of the average orientation of the adsorbates. If, in addition, the resonant vibrational transitions, as well as the resonant electronic transition, can help define the molecular axes, then the analysis to deduce molecular orientation from the measurement can be much simpler and more reliable.

The most important future application of SFG spectroscopy to surface science is, however, in the studies of transient surface phenomena. Pulsed laser probing in SFG should enable us to selectively monitor the transient species appearing on a surface, such as in a catalytic process. Free-electron lasers operating in the ir could provide the desired tunable ir beam.¹⁴ With ultrashort laser pulses, ultrafast dynamics of surface states or surface species can be studied by transient SFG. For example, one can measure the dephasing time of a vibrational mode of surface adsorbates by photon echoes: two consecutive ir pulses excite a vibrational resonance; the resultant echo can be detected by up-conversion to the visible using SFG. Since the dephasing time of a typical surface vibrational mode is expected to be around a few picoseconds or less, subpicosecond tunable ir laser pulses may be needed. We are presently working in our laboratory to demonstrate the possibility of observing such surface photon echoes.

We have shown in this paper that surface SFG can indeed be used for surface spectroscopy in the ir. The experiment reported here is the first important step that could lead to a new, exciting surface spectroscopic technique with very high time, space, and spectral resolution, and capable of studying ultrafast molecular dynamics and transient phenomena at various types of interfaces.

We gratefully acknowledge initial contributions from H. W. K. Tom and Ralph H. Page on this project, Hans Hagemann, Steve Vodor, and Andrew P. Trapani for coumarin 504 spectra, and Yili Guo for experimental assistance. H. S. acknowledges financial support from Deutsche Forschungsgemeinschaft. This work was supported by the Director, Office of Energy Research, Office

TABLE I. Parameters characterizing the vibrational resonances obtained from theoretical fit to the experimental result of sum frequency generation. The numbers in the parentheses are less accurate since they were deduced from resonance peaks appearing outside our laser tuning range.

Mode frequency solid (cm^{-1})	Halfwidth Γ_S solid (cm^{-1})	Mode frequency ω_S surface (cm^{-1})	Resonant nonlinear polarizability $\alpha_S^{(2)} = A_S/\Gamma_S$ (10^{-29} esu)	Resonant surface nonlinear susceptibility $\chi_S^{(2)} = N_S \alpha_S^{(2)}$, $N_S = 2 \times 10^{14}/\text{cm}^2$ (10^{-14} esu)
922	6	(918)	(7.0 ± 1.0)	(1.4 ± 0.2)
948	6	951	3.0 ± 0.5	0.6 ± 0.1
1050	4	1039	8.9 ± 1.0	1.8 ± 0.2
1078	5	(1074)	(5.1 ± 2.0)	(1.0 ± 0.4)
1090	5	(1087)	(10.2 ± 3.0)	(2.0 ± 0.6)
Nonresonant background			11.6 ± 1.0	2.3 ± 0.2

of Basic Energy Sciences, Materials Sciences Division of the U. S. Department of Energy under Contract No. DE-AC03-76SF00098.

*Permanent address: Physikalisches Institut der Universität Heidelberg, Heidelberg, Federal Republic of Germany.

¹See, for example, *Vibrational Spectroscopy of Adsorbates*, edited by R. F. Willis, Springer Series in Chemical Physics, Vol. 15 (Springer, Berlin, 1980); *Surface Studies with Lasers*, edited by F. R. Aussenegg, A. Leitner, and M. E. Lippitsch, Springer Series in Chemical Physics, Vol. 33 (Springer, Berlin, 1983).

²H. Ibach and D. L. Mills, *Electron Energy Loss Spectroscopy and Surface Vibrations* (Academic, New York, 1982).

³F. Traeger, H. Coufal, and T. J. Chuang, *Phys. Rev. Lett.* **49**, 1720 (1982).

⁴T. J. Chuang, *J. Electron Spectrosc. Relat. Phenom.* **29**, 125 (1983).

⁵J. P. Heritage and D. L. Allara, *Chem. Phys. Lett.* **74**, 507 (1980).

⁶See, for example, T. F. Heinz, H. W. K. Tom, and Y. R. Shen, *Laser Focus* **19**, 101 (1983); Y. R. Shen, *J. Vac. Sci. Technol. B* **3**, 1464 (1985), and references therein.

⁷C. V. Shank, R. Yen, and C. Hirliman, *Phys. Rev. Lett.* **51**, 900 (1983).

⁸An initial attempt of such an experiment was reported by H. W.

K. Tom, Ph.D. thesis, University of California, Berkeley, 1984 (unpublished).

⁹See, for example, Y. R. Shen, *The Principles of Nonlinear Optics* (Wiley, New York, 1984), Chap. 25.

¹⁰See, for example, Y. R. Shen, Ref. 9, Chaps. 2 and 10. We use the following representative values: infrared dipole moment $\sim 5 \times 10^{-19}$ esu, Raman scattering cross section $\sim 1 \times 10^{-29}$ sr⁻¹cm², vibrational linewidth $\Gamma \sim 5$ cm⁻¹.

¹¹For liquid deposition techniques, see, for example, P. K. Hansma and R. V. Coleman, *Science* **184**, 1369 (1974); P. K. Hansma, *Phys. Rep.* **30**, 145 (1977); J. P. Heritage and D. L. Allara, *Chem. Phys. Lett.* **74**, 507 (1980); J. T. Hall and P. K. Hansma, *Surf. Sci.* **71**, 1 (1978).

¹²K. B. Widors, V. A. Walters, K. N. Wang, and S. D. Colson, *J. Phys. Chem.* **88**, 6067 (1984); A. Campion and D. R. Mullins, in *Surface Studies with Lasers*, edited by F. R. Aussenegg, A. Leitner, and M. E. Lippitsch (Springer, Berlin, 1983), p. 36.

¹³T. F. Heinz, H. W. K. Tom, and Y. R. Shen, *Phys. Rev. A* **28**, 1883 (1983).

¹⁴See, for example, *Phys. Today* **37** (No. 11), 21 (1984).